Inclusion of Neutral and Anionic Guests within the Cavity of π-Metalated Cyclotriveratrylenes

K. Travis Holman,[†] Martha M. Halihan,[†] Silvia S. Jurisson,*[,†] Jerry L. Atwood,*[,†] Robert S. Burkhalter,[‡] Andrew R. Mitchell,[§] and Jonathan W. Steed*[,§]

Contribution from the Departments of Chemistry, University of Missouri—Columbia, Columbia, Missouri 65211, University of Alabama, Tuscaloosa, Alabama 35487, and King's College London, Strand, London WC2R 2LS, UK

Received May 16, 1996[⊗]

Abstract: Treatment of the chloride bridged species $[\{M(L)Cl(\mu\text{-}Cl)\}_2]$ (M = Ru, L = 4-$MeC_6H_4CHMe_2$, C_6H_6, or C_6Me_6; M = Ir, L = C_5Me_5) with silver salts AgX (X = BF_4, CF_3SO_3, CF_3CO_2 *etc.*) followed by reflux with the bowl-shaped macrocycle cyclotriveratrylene (CTV) results in the clean formation of mono-, di-, and trimetallic CTV complexes $[\{M(L)\}_n(CTV)]X_{2n}$ (n = 1, 2, 3). Further salts (X = ReO_4^-, I^-) may be generated by anion metathesis. All three types of complex display novel host−guest properties. In the case of the monometallic hosts the disruption of the characteristic columnar packing mode of the CTV, a result of the presence of the metal center, leads to the inclusion of neutral and anionic guest species (NO_2Me, Et_2O, $H\{CF_3CO_2\}_2^-$, *etc.*) within the CTV cavity. For complexes where n = 2 or 3 the inclusion of anionic guests is invariably observed. The extent of anion binding has been established by means of X-ray crystal structure determinations upon various di- and trimetallic species containing BF_4^-, $CF_3SO_3^-$, or ReO_4^-, by radiotracer analysis in solution using $^{99m}TcO_4^-$ and $^{188}ReO_4^-$, and by cyclic voltammetry. The trimetallic complex $[\{Ir(Cp^*)\}_3(CTV)][BF_4]_6$ (**9a**) in particular exhibits F···C_{CTV} contacts as short as 2.78(3) Å. The dimetallic host $[\{Ru(\eta^6\text{-}4\text{-}MeC_6H_4CHMe_2)\}_2(\eta^6\text{:}\eta^6\text{-}CTV)]^{4+}$ (**4**) is shown to have a specific affinity for large tetrahedral anions and will selectively extract both $^{99}TcO_4^-$ and ReO_4^- from aqueous solution, even in the presence of a large excess of Cl^-, $CF_3SO_3^-$, NO_3^-, SO_4^{2-}, and to some extent ClO_4^-.

Introduction

The inclusion of cations and neutral molecules within macrocyclic cavities is a well-explored and increasingly important field.[1,2] The analogous supramolecular chemistry of anions,[3] however, is relatively undeveloped, in part due to the difficulty in designing appropriate cationic or Lewis acidic receptors.[4] The synthesis of receptors which are capable of the non-covalent binding of anionic guests is, however, of considerable interest in the context of detection and removal of environmental contaminants such as nitrate and phosphates,[5] or in the nuclear industry $^{99}TcO_4^-$, for example,[6] from waste water streams. Also, applications in the inhibition of metabolic processes by complexation of the polyphosphate residues of ATP[7] or influence on phosphate transfer mechanisms[8a] may be envisaged.

Recent X-ray crystal structure determinations have demonstrated that recognition and transport of mono- and dibasic phosphate and sulfate anions in biological systems is achieved *via* a complex network of 7−12 hydrogen bonding interactions per anion. The anionic guests themselves are found to be deeply embedded within the binding protein.[8] While hydrogen bonding hosts have been applied with some success in synthetic systems,[3] we have developed an entirely new class of anion complexation hosts based upon organometallic compounds of calix[n]arenes (n = 4, 5) in which the build up of partial positive charge upon

[†] University of Missouri—Columbia.
[‡] University of Alabama.
[§] King's College London.
[⊗] Abstract published in *Advance ACS Abstracts,* September 1, 1996.

(1) (a) Pedersen, C. J. *Angew. Chem., Int. Ed. Engl.* **1988**, *27*, 1021. (b) Mertes, K. B.; Lehn, J.-M. Multidentate Macrocyclic and Macropolycyclic Ligands. In *Comprehensive Coordination Chemistry*; Wilkinson,G., Gillard, R., McCleverty, J. A., Eds.; Pergamon: Oxford, 1987; Vol. 2, pp 915−957. (c) Lehn, J.-M. *Angew. Chem., Int. Ed. Engl.* **1988**, *27*, 89.

(2) (a) Atwood, J. L. In *Cation Binding by Macrocycles*; Inoue,Y., Gokel, G. W., Eds.; Dekker: New York, 1991. (b) Shinkai, S.; Koreshi, H.; Ueda, K.; Arimura, T.; Manabe, O. *J. Am. Chem. Soc.* **1987**, *109*, 6371. (c) Bott, S. G.; Coleman A. W.; Atwood, J. L. *J. Am. Chem. Soc.* **1986**, *108*, 1709. (d) Gutsche, C. D.; Nam, K. C. *J. Am. Chem. Soc.* **1988**, *110*, 6153.

(3) (a) Bianchi, A.; Bowman-James, K.; Garcia-España, E., Eds. *Supramolecular Chemistry of Anions*; VCH: Weinheim, in press. (b) Dietrich, B. *Pure Appl. Chem.* **1993**, *7*, 1457. (c) Katz, H. E. In *Inclusion Chemistry*; Atwood, J. L., Davies, J. E. D., MacNicol, D. D., Eds.; Oxford University Press: Oxford, 1991; Vol 4, Chapter 9, pp 391−405. (d) Pierre, J.-L.; Baret, P. *Bull. Soc. Chim. Fr.* **1983**, 367. (e) Izatt, R. M.; Pawlak, K.; Bradshaw, J. S.; Bruening, R. L. *Chem. Rev.* **1991**, *91*, 1721. (f) Dietrich, B. In *Inclusion Chemistry*; Atwood, J. L., Davies, J. E. D., MacNicol, D. D., Eds.; Academic Press: London, 1984; Vol 2, Chapter 10, pp 373−405.

(4) Recently reported examples include: (a) Worm, K.; Schmidtchen, F. P.; Schier, A.; Schafer, A.; Hesse, M. *Angew. Chem., Int. Ed. Engl.* **1994**, *33*, 327. (b) Bencini, A.; Bianchi, A.; Dapporto, P.; Garcia-España, E.; Micheloni, M.; Paoletti, P.; Paoli, P. *J. Chem. Soc., Chem. Commun.* **1990**, 753. (c) Bencini, A.; Bianchi, A.; Dapporto, P.; Garcia-España, E.; Micheloni, M.; Ramirez, J. A.; Paoletti, P.; Paoli, P. *Inorg. Chem.* **1992**, *31*, 1902. (d) Yang, X.; Knobler, C. B.; Zheng, Z.; Hawthorne, M. F. *J. Am. Chem. Soc.* **1994**, *116*, 7142. (e) Beer, P. D.; Hesek, D.; Kingston, J. E.; Smith, D. K.; Stokes, S. E.; Drew, M. G. B. *Organometallics* **1995**, *14*, 3288.

(5) (a) Rudkevich, D. M.; Verboom, W.; Reinhoudt, D. N. *J. Org. Chem.* **1994**, *59*, 3683. (b) Beer, P. D.; Chen, Z.; Goulden, A. J.; Graydon, A.; Stokes, S. E.; Wear, T. *J. Chem. Soc., Chem. Commun.* **1993**, 1834. (c) Rudkevich, D. M.; Brzozka, Z.; Palys, M.; Visser, H. C.; Verboom, W.; Reinhoudt, D. N. *Angew. Chem., Int. Ed. Engl.* **1994**, *33*, 467. (d) Rudkevich, D. M.; Verboom, W.; Brzozka, Z.; Palys, M. J.; Stauthamer, W. P. R. V.; van Hummel, G. J.; Franken, S. M.; Harkema, S.; Engbersen, J. F. J.; Reinhoudt, D. N. *J. Am. Chem. Soc.* **1994**, *116*, 4341. (e) Gymer, R. G. *Chemistry: An Ecological Approach*, Harper and Row: New York, 1973. (f) Sfriso, A.; Pavoni, B.; Marcomini, A.; Raccanelli, S.; Orio, A. A. *Environ. Technol.* **1992**, *13*, 473. (g) Sfriso, A.; Pavoni, B. *Environ. Technol.* **1994**, *15*, 1. (h) Mason, C. F. *Biology of Freshwater Pollution*, 2nd ed.; Longman: Harlow, 1991.

(6) (a) Kubota, M. *Radiochim. Acta* **1993**, *63*, 91. (b) Holm, E. *Radiochim. Acta* **1993**, *63*, 57. (c) Del Cul, G. D.; Bostick, W. D.; Trotter, D. R.; Osborne, P. E. *Sep. Sci. Technol.* **1993**, *28*, 551.

(7) (a) Knowles, J. R. *Annu. Rev. Biochem.* **1980**, *49*, 877. (b) Hosseini, M. W.; Lehn, J.-M. *J. Chem. Soc., Chem. Commun.* **1988**, 397.

(8) (a) Luecke, H.; Quiocho, F. A. *Nature* **1990**, *347*, 402. (b) He, J. J.; Quiocho, F. A. *Science* **1991**, *251*, 1479. (c) Quiocho, F. A. *Philos. Trans. R. Soc. London, Ser. B* **1990**, *326*, 341. (d) Pflugrath, J. W.; Quiocho, F. A. *Nature* **1985**, *314*, 257.

S0002-7863(96)01655-1 CCC: $12.00

Scheme 1. Synthesis of New Host Complexes[a]

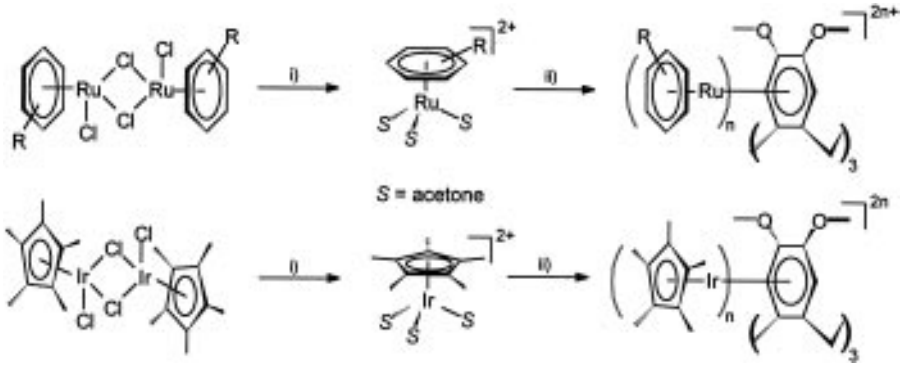

[a] (i) Excess AgX, acetone. (ii) 1/*n* CTV, reflux tfa.

the metal coordinated aromatic rings of hosts such as [{Ru(η^6-arene)}$_4$(calix[4]arene-2H)]$^{6+}$ results in the extremely deep inclusion of appropriately sized anions within the host bowl-shaped molecular cavity.[9] We now report the extension of these studies to related species based upon the trimeric macrocycle cyclotriveratrylene (2,3,7,8,12,13-hexamethoxy-5,10-dihydro-15*H*-tribenzo[*a*,*d*,*g*]cyclononene, CTV) which also possesses a shallow bowl- or saucer-shaped molecular cavity. CTV is known to form a wide variety of inclusion complexes in the solid state with guest molecules occupying extensive channels on either side of the host macrocycle.[10] The central cavity, however, is very rarely occupied by guests. Instead the CTV molecules stack in columns with the base of one saucer fitting within the cup of the one below. The only exception to this extremely characteristic packing mode is the Buckminsterfullerene complex CTV·1.5C_{60}·0.5C_7H_8 in which the CTV cavity is occupied by an enclathrated molecule of C_{60}, although even in this case additional C_{60} and toluene occupy the lattice voids in a disordered fashion.[11a]

This contribution describes the inclusion of a range of both neutral and anionic guests *within* the bowl-shaped cavity of CTV-based hosts and probes the anion binding ability of these new organometallic cations. Preliminary reports of portions of this work have already appeared.[11]

Results and Discussion

The presence of the electron donating methoxy substituents at the upper rim of the CTV cavity renders the aromatic residues particularly electron rich and therefore good potential ligands for transition metal ions such as Fe(II), Ru(II), Os(II), Co(III), Rh(III), and Ir(III) which all form stable complexes with arenes.[12] In practice, desirable properties such as stability to air and moisture, and strong M−arene bonds are more commonly associated with the second- and third-row late transition metal elements and hence we have elected to study Ru(II) and Ir(III) with the aim of obtaining stable, cationic transition metal-containing host molecules.

Synthesis of CTV Based Hosts. Organometallic host complexes were generated according to the route outlined in Scheme 1. This procedure involves treatment of the appropriate chloride-bridged species [{Ru(η^6-arene)Cl(μ-Cl)}$_2$] (arene = 4-MeC_6H_4CHMe$_2$, C_6H_6, C_6Me_6, *etc.*) or [{Ir(Cp*)Cl(μ-Cl)}$_2$] (Cp* = η^5-C_5Me_5) with a silver salt, AgX (X = BF_4, CF_3SO_3, CF_3CO_2 *etc.*), in acetone (*S*) resulting in the *in situ* formation of the solvated species [Ru(η^6-arene)(*S*)$_3$]$^{2+}$ or [Ir(η^5-Cp*)(*S*)$_3$]$^{2+}$.[13a−d] Reaction of these precursors with CTV in refluxing trifluoroacetic acid gave the following range of mono-, di-, or trimetalated compounds in good to excellent yields (see Experimental Section): [Ru(η^6-arene)(η^6-CTV)]X_2 (arene = 4-MeC_6H_4CHMe$_2$, X = BF_4 (**1a**), H(CF_3CO_2)$_2$ (**1b**), PF_6 (**1c**); arene = C_6H_6, X = BF_4 (**2a**), H(CF_3CO_2)$_2$ (**2b**); arene = C_6Me_6, X = BF_4 (**3a**), CF_3CO_2 (**3b**), CF_3SO_3 (**3c**)), [{Ru(η^6-arene)}$_2$(η^6:η^6-CTV)]X_4 (arene = 4-MeC_6H_4CHMe$_2$, X = BF_4 (**4a**), CF_3SO_3 (**4b**)), [{Ru(η^6-arene)}$_3$(η^6:η^6:η^6-CTV)]X_6 (arene = 4-MeC_6H_4CHMe$_2$, X = BF_4 (**5a**), CF_3SO_3 (**5b**); arene = C_6H_6, X = BF_4 (**6**)), and [{Ir(η^5-Cp*)}$_n$(CTV)][X]$_{2n}$ (n = 1, X = BF_4 (**7**); n = 2, X = BF_4 (**8**); n = 3, X = BF_4 (**9a**), CF_3SO_3 (**9b**)). Similarly, a mixed-metal compound [Ru(η^6-4-MeC_6H_4-CHMe$_2$){Ir(η^5-Cp*)}$_2$(η^6:η^6:η^6-CTV)][BF_4]$_6$ (**10**) was prepared by reaction of **1a** with [Ir(η^5-Cp*)(*S*)$_3$]$^{2+}$ according to Scheme 1. Schematic drawings of each newly reported complex appear in Figure 1.

In general the formation of mono-, di-, or trimetallic products was found to depend simply upon the ratio of the solvated species, [Ru(η^6-arene)(*S*)$_3$]$^{2+}$ or [Ir(η^5-Cp*)(*S*)$_3$]$^{2+}$, to CTV in the reaction mixture. Exceptions to this include the synthesis of the trimetallic species **5a** in which at least a 1.5-fold excess of chloride dimer is required in order for the reaction to proceed cleanly to the desired trimetalated product. Also, despite attempts using a large excess of starting material, complex **5b** could not be synthesized without contamination by the dimetalated complex. The two products could be easily separated, however, by fractional crystallization. Notably, it proved impossible to generate any hexamethylbenzene containing cationic hosts other than the monometallic species, **3**, under the conditions employed. In this case it seems likely that addition of more than one "Ru(C_6Me_6)$^{2+}$" moiety to the outer surface of the CTV molecule would result in severely unfavorable steric interactions between the methyl substituents of the adjacent hexamethylbenzene rings.

Interestingly, the second and third metalation steps were found to be inhibited by the presence of certain counterions; *e.g.* direct

(9) (a) Steed, J. W.; Juneja, R. K.; Atwood, J. L. *Angew. Chem., Int. Ed. Engl.* **1994**, *33*, 2456. (b) Steed, J. W.; Juneja, R. K.; Atwood, J. L. *Angew. Chem.* **1994**, *106*, 2571. (c) Steed, J. W.; Johnson, C. P.; Juneja, R. K.; Burkhalter, R. S.; Atwood, J. L. *Supramol. Chem.* **1996**, *6*, 235.

(10) (a) Steed, J. W.; Zhang, H.; Atwood, J. L. *Supramol. Chem.* **1996**, *7*, 37. (b) Zhang, H.; Atwood, J. L. *J. Crystallogr. Spectrosc. Res.* **1990**, *20*, 465. (c) Collet, A. *Tetrahedron* **1987**, *43*, 5725. (d) Cerrini, S.; Giglio, E.; Mazza, F.; Pavel, N. V. *Acta Crystallogr., Sect. B* **1979**, *35*, 2605. (e) Birnbaum, G. I.; Klug, D. D.; Ripmeester, J. A.; Tse, J. S. *Can. J. Chem.* **1985**, *63*, 3258.

(11) (a) Steed, J. W.; Junk, P. C.; Atwood, J. L.; Barnes, M. J.; Raston, C. L.; Burkhalter, R. S. *J. Am. Chem. Soc.* **1994**, *116*, 10346. (b) Holman, K. T.; Halihan, M. M.; Steed, J. W.; Jurisson, S. S.; Atwood, J. L. *J. Am. Chem. Soc.* **1995**, *117*, 7848.

(12) Wilkinson, G.; Gordon, F.; Stone, A.; Abel, E. W., Eds. *Comprehensive Organometallic Chemistry*; Pergamon: Oxford, 1982.

(13) (a) Bennett, M. A.; Matheson, T. W. *J. Organomet. Chem.* **1979**, *175*, 87. (b) Bennett, M. A.; Smith, A. K. *J. Chem. Soc., Dalton Trans.* **1974**, 233. (c) Kang, J. W.; Moseley, K.; Maitlis, P. M. *J. Am. Chem. Soc.* **1969**, *91*, 5970. (d) White, C.; Maitlis, P. M. *J. Chem. Soc. A* **1971**, 3322. (e) Rybinskaya, M. I.; Kudinov, A. R.; Kaganovich, V. S. *J. Organomet. Chem.* **1983**, *246*, 279.

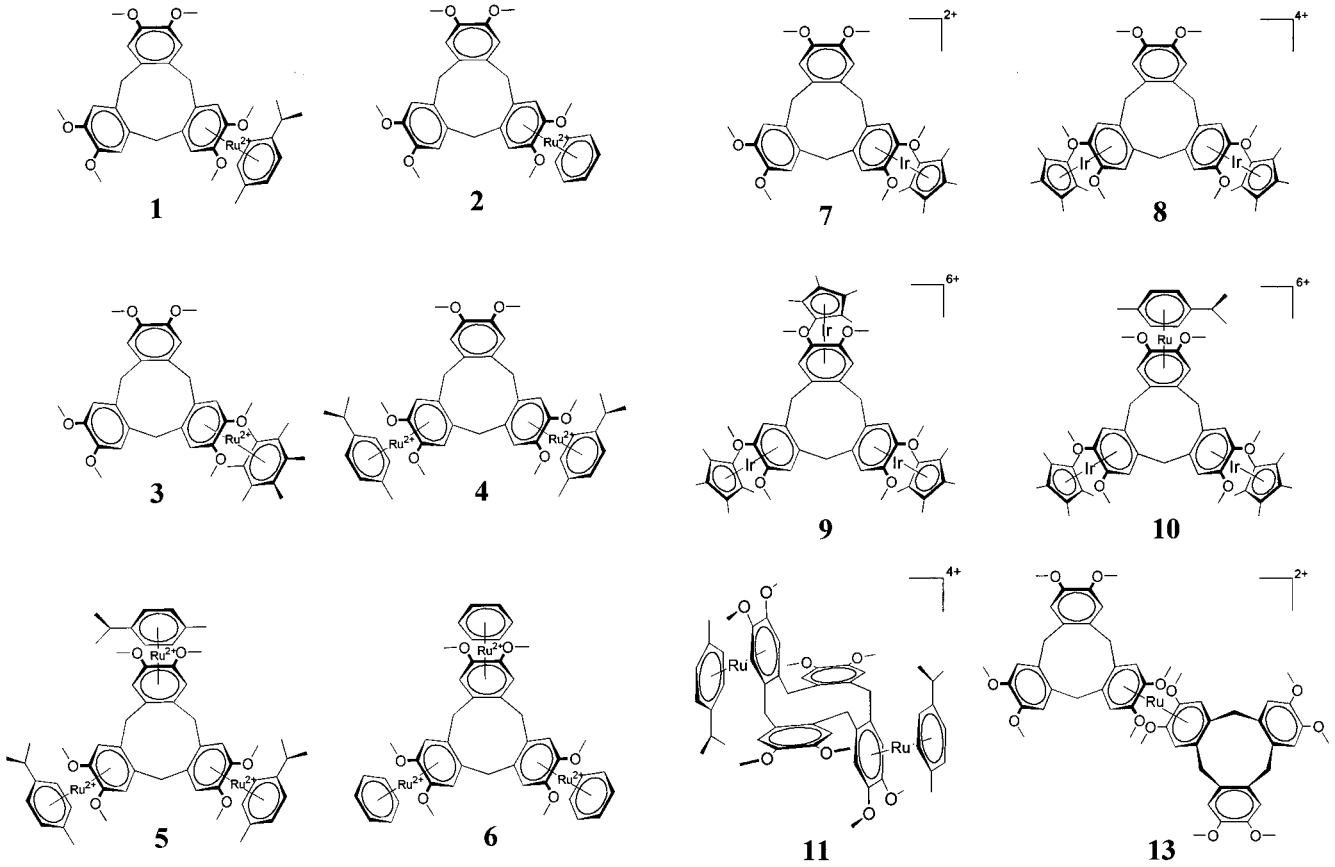

Figure 1. Schematic representation of the newly prepared cations.

reaction of a large excess of [{Ru(η^6-4-$MeC_6H_4CHMe_2$)Cl(μ-Cl)}$_2$] with CTV in refluxing CF_3CO_2H without treatment with silver salt, according to the method of Rybinskaya *et al.*,[13e] results in a monometallic complex, namely **1b,** not the di- or trimetallic species. We have also noted this effect in our work on calix[4]arene-based hosts where the tetrametallic species [{Ru(*p*-cymene)}$_4$(calix[4]arene-2H)]X_6 ($X = BF_4^-$, $CF_3SO_3^-$, HSO_4^-) may be readily synthesized according to Scheme 1, but no more than two metal centers may be added to the calix[4]arene when phosphates, chloride, tungstate, acetate or trifluoroacetate are present as principal counterions. Consequently, compounds of type [{Ru(*p*-cymene)}$_2$(calix[4]arene-H)]$^{3+}$ are isolated.[9a,14] This phenomenon may well be a kinetic effect arising from close ion pairing with, or coordination of, more strongly ligating anions, resulting in a relatively bulky "solvated" precursor which undergoes steric repulsions with the initially formed monometalated CTV derivative. Indeed, the PF_6^- anion is known to undergo partial hydrolysis at room temperature in the presence of the tris acetone complex [Ru(η^6-arene)-$(OCMe_2)_3$]$^{2+}$ to give mainly mesityl oxide and [$Ru_2(\mu$-$PO_2F_2)_3$-(η^6-arene)$_2$]$^+$ *via* a coordinated ketol intermediate.[15]

Salts of anions whose conjugate acids have a pK_a greater than that of CF_3CO_2H are not directly available *via* the route outlined in Scheme 1 because of protonation by this solvent medium. A number of complexes are obtainable, however, by simple anion metathesis. [{Ru(*p*-cymene)}$_2$(CTV)][ReO_4]$_3$[CF_3SO_3] (**4c**), [{Ru(*p*-cymene)}$_2$(CTV)]I_4 (**4d**), and various phosphate containing salts have been obtained this way, although the insolubility of the phosphate salts in conventional organic solvents has made their characterization difficult.

Each new host complex has been characterized by ^{1}H NMR spectroscopy (see supporting information) while analytical data were obtained for the $[BF_4]^-$ salt of each new cation (see Experimental Section). Selected compounds were also analyzed by ^{13}C NMR spectroscopy (see supporting information), FAB mass spectrometry, IR spectroscopy, and X-ray crystallography. The ^{1}H NMR spectra of monometallic hosts **1**−**3** display the expected pattern of three singlets in the low field region for the CTV fragment, with resonances arising from the two uncoordinated rings occurring at similar chemical shifts (*e.g.* for **1a**, δ 7.33, 7.15, 7.14 ppm). This type of pattern is observed in reverse for each of the dimetallic hosts. Consistent arrangements are noted for the methylenic and methoxy protons in each case. The CTV fragments of the trimetallic host molecules, with the exception of **10**, display ^{1}H NMR spectra similar to that of the free ligand with significant chemical shift differences ($\Delta\delta$ 0.17−0.75 ppm). In the ^{1}H NMR spectrum of the mixed-metal complex **10** the protons of the CTV rings give rise to two resonances in the ratio 2:1 (δ 7.63, 7.37 ppm) assigned to the Ir and Ru coordinated CTV decks, respectively. The higher chemical shift of the iridium containing part of the cation is consistent with the results observed for **5** and **9**.

In almost all cases evidence was noted for the presence of included solvent molecules. For example, the ^{1}H NMR spectrum of **1a** (recrystallized from CF_3CO_2H/Et_2O vapor diffusion) exhibited a broad signal at δ 2.31 ppm assigned to water and resonances at δ 1.16 (t) and 3.46 (q) assigned to diethyl ether, even after drying, consistent with the results of the X-ray crystal structure of this complex (*vide infra*). The Nujol mull infrared spectrum exhibited a strong, broad band at 3480 cm^{-1} assigned to water of crystallization.

The positive ion FAB mass spectrum of **1a** exhibited a strong molecular ion peak at *m/z* 687 as well as a smaller signal at *m/z* 773 corresponding to the cation in association with one tetrafluoroborate anion. Similarly **2a** displayed peaks at *m/z* 630 and 717. For the dimetallic host **4a** signals centering on *m/z* 919, 1007, 1093, and 1182 were clearly observed corre-

(14) Steed, J. W.; Atwood, J. L. Manuscript in preparation.
(15) Bennett, M. A.; Matheson, T. W.; Robertson, G. B.; Steffen, W. L.; Turney, T. W. *J. Chem. Soc., Chem. Commun.* **1979**, 32.

Table 1. Crystal Data for New Compounds[a]

compd	**1a**	**1b**	**3b**	**5a**	**8**	**9a**	**13**
formula	$C_{41}H_{55.4}O_{7.7}B_2F_8Ru$	$C_{45}H_{46}O_{14}F_{12}Ru$	$C_{46}H_{57}F_6N_3O_{16}Ru$	$C_{57}H_{72}B_6F_{24}O_8Ru_3$	$C_{54}H_{60}B_4F_{16}O_7Ir_2$	$C_{57.5}H_{78.5}O_{8B6}F_{24}Ir_3$	$C_{60}H_{78}O_{24}B_2F_8N_6Ru$
fw (g mol^{-1})	938.49	1139.89	1123.02	1709.22	1552.66	2002.17	1541.99
space group	$P2_1/a$	$P2_1/n$	$P2_1/n$	$Pa\bar{3}$	$P2_1/n$	$C2/c$	$P2_1/c$
a (Å)	10.239(2)	19.768(6)	16.157(3)	25.173(2)	14.799(4)	27.125(6)	15.345(6)
b (Å)	22.003(10)	12.2399(13)	18.948(3)	25.173(2)	19.250(2)	15.4168(14)	11.917(5)
c (Å)	19.341(2)	21.834(6)	16.509(2)	25.173(2)	23.927(7)	37.118(9)	21.801(10)
α (deg)	90.0	90.0	90.0	90.0	90.0	90.0	90.0
β (deg)	97.43(1)	112.89(1)	96.66(1)	90.0	95.72(1)	100.38(1)	109.71(2)
γ (deg)	90.0	90.0	90.0	90.0	90.0	90.0	90.0
V (Å^3)	4321(7)	4867(2)	5020(1)	15952(2)	6782(3)	15268(5)	3753(3)
Z	4	4	4	8	4	8	2
D_c (g cm^{-3})	1.45	1.56	1.49	1.42	1.52	1.74	1.37
μ(Mo Kα) (cm^{-1})	4.37	4.32	33.50[f]	6.60	40.07	53.21	2.95
F(000)	1892	2320	2320	6848	3032	7744	1684
crystal size (mm)	0.5 × 0.4 × 0.1	0.15 × 0.20 × 0.25	0.4 × 0.3 × 0.05	0.5 × 0.3 × 0.1	0.2 × 0.35 × 0.2	0.2 × 0.3 × 0.2	0.8 × 0.6 × 0.2
max 2θ (deg)	46	46	120[f]	50	46	45	50
no. of reflcns collected	6564	6982	7759	5357	9818	10366	7218
no. of independent refcns	5122	6756	7459	4694	9400	9907	5872
no. of observed reflcns, $I > 2\sigma(I)$	3838[c]	3230	5057	1853	6395	6993	4927[c]
crystal decay	no	−16% (corr)	−7% (corr)	−34% (corr)	−2.9% (corr)	−13% (corr)	−2%
refinement method[b]	F	F^2	F^2	F^2	F^2	F^2	F
parameters	527	592	630	316	772	940	457
R, R_w or $wR2$ (observed data)	0.078, 0.084	0.052, 0.119	0.095, 0.241	0.082, 0.226	0.053, 0.143	0.058, 0.171	0.054, 0.079
R, wR_2 (all data)[d]		0.153, 0.135	0.125, 0.268	0.223, 0.294	0.100, 0.161	0.103, 0.212	
largest residual peak (e Å^{-3})	0.71	0.76	2.19[e]	0.95	2.49[e]	2.12[e]	0.52

[a] Mo Kα radiation, $\lambda = 0.71069$ Å; temperature 20 °C. [b] Full matrix least squares on either F or F^2. [c] $I > 3\sigma(I)$. [d] Structures refined using SHELXL-93.[14] [e] Close to one of the metal atoms. [f] Cu Kα radiation.

sponding to the molecular cation itself and in association with 1−3 tetrafluoroborate anions respectively. For the trimetallic host **5a** peaks are observed for the cation in association with three, four, and five anions (*m/z* 1417, 1503, 1592). For **6** peaks are only observed corresponding to the cation in association with one and two anions (*m/z* 1078, 1164), whereas **10** demonstrated peaks at *m/z* 1341, 1515, 1602, 1689, 1776 corresponding to the cation and it in association with 2−5 tetrafluoroborate anions. In all cases isotope distribution patterns matched those expected for the various combinations of the naturally occurring isotopes of the relevant atoms (calculations based on ^{102}Ru, ^{193}Ir, and ^{11}B).

Solid State Studies. The solid state structures of the new host−guest systems presented here were probed, whenever possible, by X-ray crystallography. Crystal data are given in Table 1, while tables of atomic coordinates, bond lengths and angles, thermal parameters, and H-atom coordinates have been deposited as supporting information.

(a) Monometallic hosts. Complex **1a** crystallizes as a diethyl ether/water solvate **1a**·Et_2O·0.7H_2O. The structure of the cation is shown in Figure 2 along with the included molecule of diethyl ether. The structure consists of the expected CTV unit with the cyclononatriene ring in the usual crown conformation,[10] capped on one face by the "Ru(4-MeC_6H_4CHMe_2)$^{2+}$" moiety. Inter-ring centroid separations within the macrocycle fall in the range 4.75−4.83 Å, similar to those found in the free ligand (4.70−4.96 Å), although the conformation of the CTV moiety is somewhat closer to the ideal C_{3v} symmetry. The Ru−C distances of these complexes are consistently grouped into two distinct sets with longer bonds to the methoxy substituted carbon atoms. In this case, Ru−C(3,4) bonds average 2.33(1) Å, *cf.* Ru−C(1,2,5,6) 2.21(1) Å (av). The water molecule, which is of fractional occupancy, lies bridging a pocket formed by both tetrafluoroborate anions and the *p*-cymene ring. The CTV cavity includes a molecule of diethyl ether situated in a highly disordered fashion near the metalated ring A (O(1S)···C(3A) 3.26(3) Å) and there again exists the possibility of a weak interaction between the solvent oxygen atom and the coordinated CTV ring.

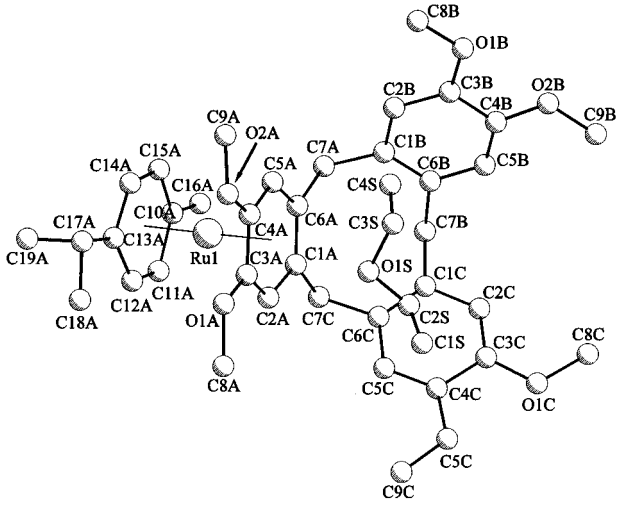

Figure 2. X-ray crystal structure of the monometallic host **1a** showing the included molecule of diethyl ether and the adopted labeling scheme.

Crystals of the same cation in association with two hydrogen ditrifluoroacetate anions (**1b**) were isolated from the direct reaction of excess chloride dimer with CTV according to the method of Rybinskaya *et al.*[13e] The cation adopts the same conformation as in **1a** with inter-ring centroid separations falling in the range 4.62−4.86 Å. The anions form strongly interacting dimers with a transoid conformation and the oxygen atoms approximately coplanar. The O···O hydrogen bonding distances are 2.47(1) and 2.45(1) Å. The host cavity is occupied by the hydrophobic trifluoromethyl substituent of one of the dimeric H(CF_3CO_2)$^-$ anions (Figure 3). This facilitates an interesting

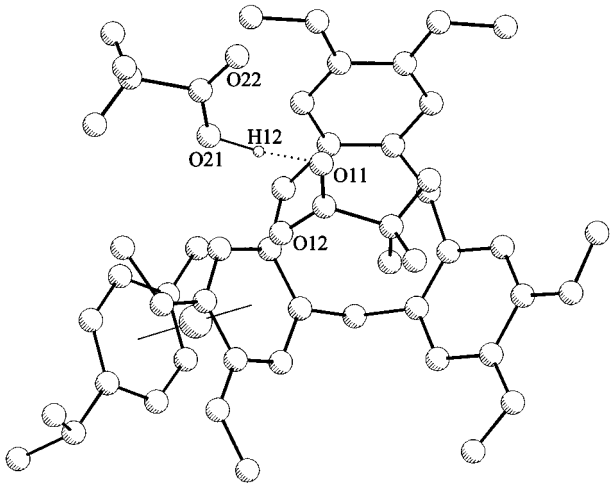

Figure 3. Inclusion of $[H(CF_3CO_2)_2]^-$ by the monometallic host **1**.

form of anion−cation interaction involving the carbonyl oxygen atom pointing down toward the metalated ring of the macrocycle. The O−C_{CTV} nonbonded contacts (O(12)···C(4A) 2.89(2) Å and O(12)···C(5A) 3.05(2) Å) suggest that this electrostatic interaction, along with the hydrophobic van der Waals type attraction involving the trifluoromethyl moiety, is the likely driving force for the inclusion. Other anion−cation contacts are above 3.11 Å.

Crystallization of the analogous monometallic hexamethylbenzene derivative 3**b** from nitromethane/diethyl ether resulted in the inclusion complex $[Ru(\eta^6\text{-}C_6Me_6)(\eta^6\text{-CTV})][CF_3CO_2]_2\cdot 3NO_2Me$ with discrete, rather than dimeric, trifluoroacetate anions. The X-ray crystal structure of this material reveals a more conventional range of supramolecular interactions in which the trifluoroacetate anions are positioned to either side of the metal center, while the CTV cavity and other voids in the lattice are occupied by the nitromethane solvent molecules. The hydrophobic methyl substituent of the nitromethane solvent molecule is situated in the more hydrophobic portion of the cavity, while the polar oxygen atoms are involved in a charge-dipole interaction and are centered above the metalated ring (A) with close contacts of O(1S)···C(4A) 3.19(1) Å and O(2S)···C(2A) 3.19(1) Å.

(b) Bimetallic Hosts. The binuclear ruthenium complex **4b** was also characterized by X-ray crystallography as reported previously.[11b] The dimensions of the molecular cavity are similar to those of the monometalated hosts with a relatively short centroid−centroid separation of 4.69 Å between the two metalated rings and longer separations of 4.72 and 4.89 Å to the uncoordinated aromatic residue. As noted for the monometalated hosts both metal centers exhibit longer bonds to the carbon atoms bearing methoxy substituents, C(3) and C(4), than the remaining four (2.353(8) Å *vs* 2.200(7) Å av). Most importantly, the structure determination demonstrates that one of the triflate anions is located directly within the cavity of the macrocycle (Figure 4) with the sulfonato head group pointing directly between the two metalated rings while the hydrophobic $-CF_3$ substituent occupies the center of the cavity. The closest sulfonate oxygen atom to host contact, O(2)···C(2B), of 2.95(1) Å is relatively long in comparison to F···C distances as low as 2.85 Å observed for the calixarene complex $[\{Ru(p\text{-cymene})\}_4(\text{calix[4]arene-2H})][BF_4]_6$ (although much shorter than those for the lattice triflate anions) because of the presence of only two metal centers. The rigidity with which the anion is held within the cavity is clearly reflected, however, in the crystallographic thermal parameters which are all markedly smaller than those for the other three triflate anions. This indicates the sterically restricted nature of the intracavity site.

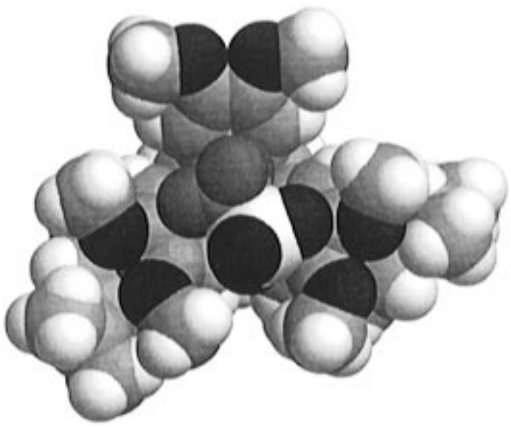

Figure 4. Space-filling view of $[CF_3SO_3]^-$ inclusion by the bimetallic host **4b**.

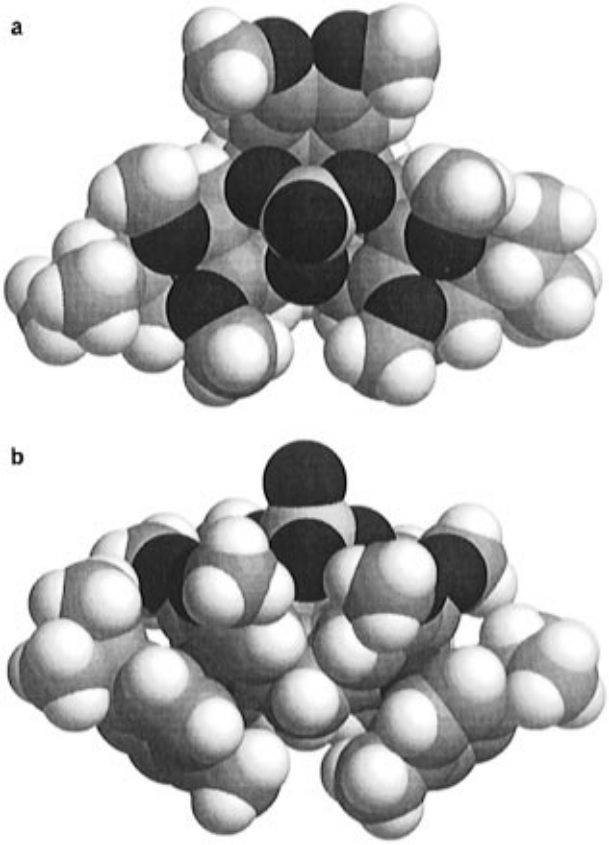

Figure 5. Space-filling plot of the perrhenate complex **4c** showing the size compatibility between the guest and host: (a) top view, (b) side view.

In the crystal, the host molecules pack in a columnar array separated by the included triflate anion.

Slow crystallization of **4b** in the presence of 2 equiv of $[N^nBu_4][ReO_4]$ resulted in the isolation of crystals of the mixed perrhenate/triflate salt $[\{Ru(\eta^6\text{-}p\text{-cymene})\}_2(\eta^6\text{:}\eta^6\text{-CTV})][ReO_4]_3\text{-}[CF_3SO_3]\cdot NO_2Me$ (**4c)** which has also been characterized by X-ray crystallography.[11b] The structure clearly demonstrates the inclusion of a perrhenate anion in place of the triflate anion within the CTV cavity. The included anion is situated slightly off the pseudo 3-fold axis of the CTV moiety toward the metalated rings in a "three down" fashion with the oxygen atoms nesting between the carbocyclic rings. The space-filling model of this complex demonstrates the excellent size and shape complimentarity between the host and the bound anionic guest (Figure 5). The inclusion of this particular anion is of exceptional interest since it is a structural model for the environmental contaminant $^{99}TcO_4^-$. Preliminary radiotracer

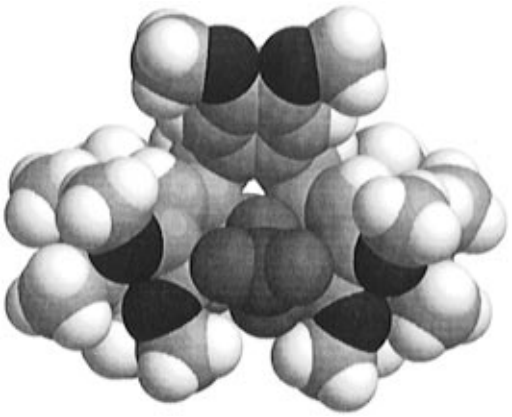

Figure 6. Space-filling representation of the bimetallic iridium species **8** showing the included $[BF_4]^-$ anion.

studies have shown that this host demonstrates a marked affinity for this anion (*vide infra*).[11b]

The iridium-based, dimetallic host **8** was crystallized as the diethyl ether solvate by slow diffusion of diethyl ether into a nitromethane solution of the complex. The presence of diethyl ether was confirmed by the ^{1}H NMR spectrum of the complex which suggested *ca.* two molecules of solvent per host molecule, in agreement with the crystallographically determined value. The structure of **8** is broadly similar to its ruthenium analogue **4**, with the CTV ligand exhibiting C_s symmetry (intercentroid separations of 4.58−4.98 Å) and relatively long bonds from the metal center to the methoxy substituted carbon atoms C(3) and C(4). As anticipated, one of the four $[BF_4]^-$ anions occupies the intracavity site (Figure 6), orientated in a similar fashion as the triflate ion in **4b** with one of the fluorine atoms pointing between the two coordinated decks of the CTV ligand. The other three fluorine atoms are disordered around the B(1A)−F(1A) axis, suggesting that the included anion is free to rotate within the cavity about the B(1A)−F(1A) axis. This result is consistent with the poor size match between $[BF_4]^-$ and the CTV cavity also observed for the trimetalated ruthenium derivative **5a** (*vide infra*). For **8** the shortest anion−host(carbon) contacts involve the included anion F(1A)···C(2B) 2.94(1) Å, F(1A)···C(3B) 2.88(1) Å, F(7A)···C(4A) 2.90(5) Å, and F(7A)···C(3A) 2.93(6) Å. The closest contact involving the extra-cavity anions occurs with one of the cyclopentadienyl ligands (F(3D)···C(11A) 2.98(2) Å).

(c) Trimetallic Hosts. In a preliminary report we also reported the X-ray crystal structure of the trimetallic species **5a**. At the time we were unable to adequately resolve the highly disordered nature of the guest species although it seemed clear that a BF_4^- anion was likely from charge balance considerations.[11a] Re-refinement of the structure on F^2 (see Experimental Section) using the program SHELXL-93[16] has resulted in a much clearer determination which is presented here. Compound **5a** crystallizes in the cubic space group $Pa\bar{3}$ with $a = 25.173(2)$ Å. The $[\{Ru(\eta^6\text{-}4\text{-}MeC_6H_4CHMe_2)\}_3(\eta^6{:}\eta^6{:}\eta^6\text{-CTV})]^{6+}$ cation is situated upon a 3-fold rotation axis such that only one third of the molecule is unique. This is in itself remarkable since previous structures of nonmetalated CTV indicate that the symmetry is generally C_s as a consequence of the interannular repulsion between the three carbocyclic rings and absence of homoaromaticity.[10] The removal of π-electron density by the transition metal centers in **5a** is sufficient to lower these repulsions to such an extent that the molecule adopts its full C_{3v} symmetry. This results in a deeper molecular cavity with intercentroid separations of 4.52 Å as opposed to much wider dimensions of 4.70−4.96 seen for free CTV[10] and **1a**.[10] Of

(16) Sheldrick, G. M. *SHELXL-93*, University of Göttingen, 1993.

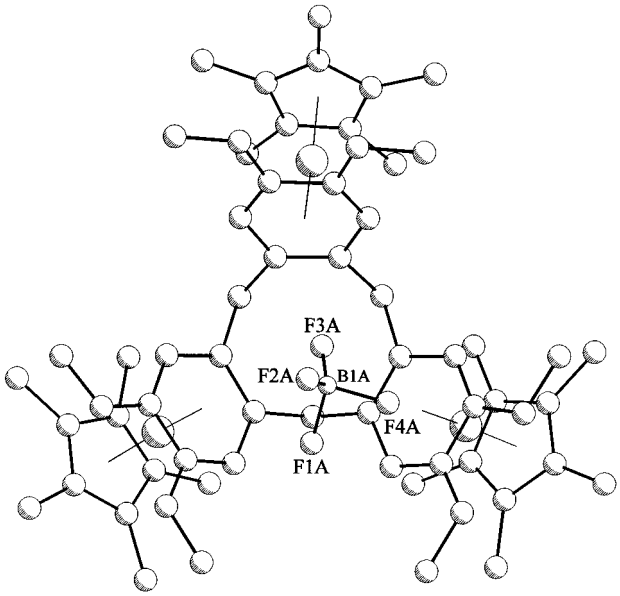

Figure 7. X-ray crystal structure of the trimetallic iridium complex **9a** with included $[BF_4]^-$ anion.

the six tetrafluoroborate anions associated with the cation three are accounted for by one full occupancy BF_4^- situated upon a general position in the crystallographic asymmetric unit. Of the remaining three, one is situated in a disordered fashion with the boron and one fluorine atom on the 3-fold rotation axis while the other two have all atoms at 33% occupancy and lie to one side of the 3-fold axis. One of these latter two anions is situated within the cavity of the metalated host molecule and it seems likely that the crystallographic disorder is caused by the highly favorable nature of this intracavity position which may only be occupied by one anion at a time. This results in the necessity of arranging the remaining five within the 3-fold crystallographic symmetry. The closest CTV−fluorine contacts fall in the range 2.94−3.11 Å and are significantly shorter than those observed for the lattice BF_4^-···*p*-cymene contacts (over 3.10 Å). These host−anion contacts are similar in magnitude to those found for the triiridium *p-tert*-butylcalix[5]arene host $[\{(Ir(Cp^*)\}_3(p\text{-}tert\text{-}butylcalix[5]arene\text{-}H)][BF_4]_5$ (2.93−3.09 Å)[9c] and reflect the poor size match between host cavity and anion. In contrast the tetraruthenium host $[\{Ru(p\text{-cymene})\}_4(calix[4]arene\text{-}2H)][BF_4]_6$ exhibits extremely tight binding of one of the BF_4^- anions with F···C contacts as low as 2.85 Å and no disorder of the guest anion.[9a,b]

Crystals of the analogous triiridium compound **9a** were also obtained. Surprisingly, however, the host cation does not exhibit C_{3v} as seen in **8**, and the crystals consequently cannot adopt the cubic packing mode. Instead, the dimensions of the CTV cavity are perturbed due to the presence of a second encroaching BF_4^- anion. This time the intracavity anion is oriented in a slanted "three-down" fashion (Figure 7) and is wedged between metalated rings A and B (cent(A)···cent(B) 4.80 Å) with very short anion−host contacts of F(1A)···C(2B) 2.92 Å and F(4A)···C(3A, 4A) 2.78(3), 2.82(3) Å, respectively. This F(4A)-C(3A) distance in particular is the shortest so far observed in these systems. The second anion is infringing upon the cavity from between Ir(2) and Ir(3) (cent(B)···cent(C) 4.70 Å, *cf.* A···C 4.90 Å). It is possible that ion pairing interactions between the two metal centers and this anion are the cause for the conformational distortion from 3-fold symmetry.

Anion Binding in Solution. Two phase (NO_2Me/saline) anion transport experiments were employed to determine the degree of ReO_4^- and TcO_4^- complexation with the host cation **4** both alone and in competition with a number of other anions. In these experiments it was demonstrated by UV-vis spectros-

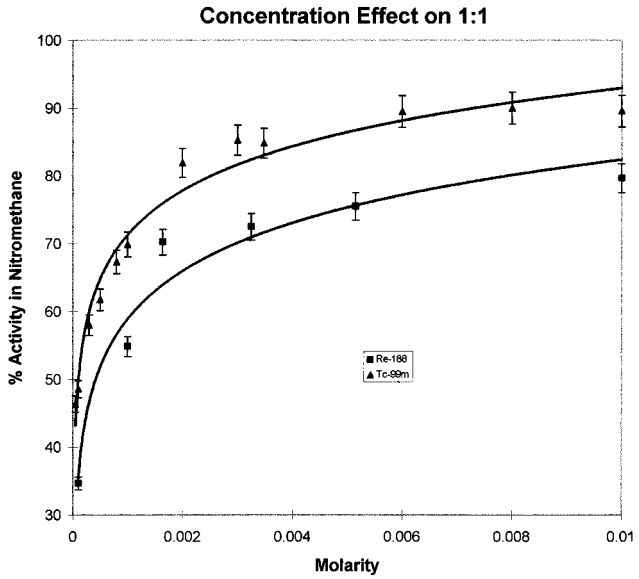

Figure 8. $^{188}ReO_4^-$ and $^{99m}TcO_4^-$ partitioning (bulk ReO_4^-) as a function of host concentration at 1:1 **4b**:ReO_4^- ratios.

copy that the host cation of **4b** essentially remains (>90%) in the organic phase, and acts as a phase transfer host with anions being extracted from the aqueous saline phase. The studies were monitored by adding $^{188}ReO_4^-$ and $^{99m}TcO_4^-$ radiotracers to the experimental solutions and all results are reported as the percentage of total activity present in the nitromethane phase after mixing.

Blank studies performed at 3.25 mM concentrations in the absence of a host cation indicated that only 7(3)% and 6(2)% of the activity is extracted into the organic phase in the case of $^{188}ReO_4^-$ and $^{99m}TcO_4^-$, respectively, while control experiments using NBu_4Cl resulted in a highly concentration dependent phase distribution, peaking at *ca.* 40% extraction into the organic phase. With **4b** present (3.25 mM, 1:1 host:anion ratio) 71-(1)% of the $^{188}ReO_4^-$ and 84(1)% of the $^{99m}TcO_4^-$ was extracted, demonstrating the selectivity of complex **4** for these anions over $CF_3SO_3^-$ and Cl^- (both present in excess). The extraction efficiency is seemingly only limited by the solubility of **4b** in the organic phase (Figure 8) and at concentrations of 10.0 mM 79(2)% and 88(2)% of the $^{188}ReO_4^-$ and $^{99m}TcO_4^-$ are partitioned into the organic phase, respectively. At lower concentrations significantly less activity was extracted (1.0 mM $^{188}ReO_4^-/^{99}TcO_4^-$: 55(1)/70(2)%). Importantly, under comparable conditions, the perrhenate radiotracer was always extracted less efficiently than the pertechnetate. This result is surprising since rhenium is commonly believed to be an excellent chemical analogue for technetium, and may result from a combination of a difference in interaction with the host cation (possibly suggesting a better size match between TcO_4^- and the host cavity in **4**) and differences in the solvation energies of the free anions. The ability of ReO_4^- to expand its coordination sphere may also be a factor.[17]

Variation of the relative concentrations of ReO_4^- with respect to **4b** showed that there was essentially no change in the partitioning of the ReO_4^- at low anion:host ratios. Conversely, as the concentration of perrhenate was increased relative to **4b**, a corresponding decrease in the activity in the organic layer was observed. Notably, this decline in extractability has its onset at approximately a 1:4 host:anion ratio which is not surprising since **4** is a tetrapositive host.

Competition studies (3.25mM **4b**, 1:1 host:ReO_4^- ratio) were performed by carrying out the partition experiments in the presence of *ca.* 20 fold excesses of sodium chloride, sulfate, nitrate, or perchlorate in order to further probe anion selectivity. Even in such large excess, only perchlorate was capable of significantly suppressing the extraction of the $^{188}ReO_4^-$ resulting in partitioning of only 6(3)% of the $^{188}ReO_4^-$ into the organic phase. Excess chloride sulfate and nitrate resulted in 70(2)%, 68(1)%, and 65(1)%, respectively. However, in the presence of a 1:1 mixture of ClO_4^-:$^{188}ReO_4^-$ the degree of ReO_4^- partitioning was virtually unaffected by the competing perchlorate, demonstrating that the host has a markedly greater affinity for ReO_4^-. As a final comparison, measurements were undertaken upon a 1:1:1 mixture of TcO_4^-:ReO_4^-:**4b**, resulting in the partitioning of 77(1)% of the ^{99m}Tc and 63(1)% of the ^{188}-Re into the organic phase. These results suggest a small selectivity of **4b** for TcO_4^- over the very similar ReO_4^-.

We conclude that, under the conditions reported herein, host **4** demonstrates a marked selectivity for large tetrahedral oxoanions with the selectivity sequence $TcO_4^- > ReO_4^- > ClO_4^- \gg NO_3^- > SO_4^{2-} > Cl^-$. The low affinity for sulfate is surprising given its similarity in size and shape to the MO_4^- anions, as well as its high negative charge. It is quite likely that significant partitioning of this anion into the organic phase is prevented by its high free energy of hydration.

Cyclic Voltammetry. The anion binding properties of host **4** (as the triflate salt) were also investigated by means of cyclic voltammetry. In the absence of any externally added anion, the cyclic voltammogram (CV) of **4** displayed two reduction waves, −670 and −825 mV (*vs* Ag/Ag^+, irreversible at scan rates of 50−200 mV s^{-1}). The potential of these two reduction waves was relatively unaffected by the addition of $[NBu_4]I$, $[NBu_4]Cl$, and $[NBu_4][BPh_4]$ (up to *ca.* 15 mV anodic shift in both reduction waves), although the appearance of a significant return wave on both peaks was noted in the case of the iodide experiment. A slight, concentration dependent, cathodic shift was noted for $[NBu_4][ReO_4]$ with the reduction wave at −825 mV especially, shifting to −809 mV. Strikingly, however, addition of the HSO_4^- anion in molar ratios increasing from 1:10 to 2:1 caused a marked change in the appearance of the CV, such that both reduction waves merged into a single, irreversible peak at −753 mV. A significant effect was also noted for the addition of $[NBu_4][H_2PO_4]$ with a net cathodic shift of 43 mV for the second reduction wave, gradually increasing over the same range of molar ratios. These results are typical of the redox potential shifts noted by Beer *et al.* for systems based upon the Co^{3+}/Co^+ couple in cobalticinium derivitaves.[4e,18]

It is difficult to interpret the significance of the direction of the shifts in reduction potential. However, the fact that the most striking effects on the CV are obtained from large, tetrahedral-like anions such as $H_2PO_4^-$ and HSO_4^- strongly supports the contention that they are bound within the macrocyclic cavity, which is of complementary dimensions to these anions, consistent with the radiochemical data reported above. While a smaller effect is noted for ReO_4^-, it is important to note the difference in solvent medium between the cyclic voltammetric and radiochemical experiments. It is highly probable that the affinity of the host for the target anions is significantly influenced by solvation effects. Thus, in saline−NO_2Me little sulfate selectivity is noted, whereas HSO_4^- exerts a strong influence in MeCN solution, as may be expected from the high

(17) (a) Deutsch, E.; Libson, K.; Vanderheyden, J.-L. In *Technetium and Rhenium in Chemistry and Nuclear Medicine 3*; Nicolini, M., Bandoli, G., Mazzi, U., Eds.; Cortina International: Verona, 1990; pp 13−22. (b) Vajo, J. J.; Aikens, D. A.; Ashley, L.; Poeltl, D. E.; Bailey, R. A.; Clark, H. M.; Bunce, S. C. *Inorg. Chem.* **1981**, *20*, 3328.

(18) (a) Beer, P. D.; Drew, M. G. B.; Hazlewood, C.; Hesek, D.; Hodacova, J.; Stokes, S. E. *J. Chem. Soc., Chem. Commun.* **1993**, 229. (b) Beer, P. D.; Hesek, D.; Hodacova, J.; Stokes, S. E. *J. Chem. Soc., Chem. Commun.* **1992**, 270.

affinity of the hydrogen sulfate anion for aqueous media. It is likely that the opposite effect is in evidence for ReO_4^-.

As a final experiment the affinity of host **4** for the large $[Re_2Cl_8]^{2-}$ anion was investigated. Extremely large shifts of *ca.* 200 mV in both reduction waves were observed with irreversible reductions occurring at −472 and −625 mV. The significant effect of this anion in particular may well be attributable to its higher negative charge, suggesting a significant electrostatic contribution to the binding, and good size match of at least one end of the $Re_2Cl_8^{2-}$ anion, with the CTV cavity.

Reactions with Cyclotetraveratrylene (CTTV). Under carefully controlled conditions the acid catalyzed condensation of veratryl alcohol (3,4-dimethoxybenzyl alcohol) with formaldehyde yields up to *ca*. 30% of the cyclic tetramer cyclotetracatechylene (CTTV) as well as CTV (which forms the bulk of the yield).[10c,19] In solution the CTTV molecule is fluxional, alternating between a chair conformation and a shallow bowl.[19] In the solid state, however, the chair conformation is invariably observed.[20,21] Attempts to stabilize the bowl conformation by demethylation of the methoxy substituents to give the related catechol derivative cyclotetracatechylene resulted in an octol which still exhibited a chair conformation in the solid state.[22] We reasoned, however, that addition of bulky organometallic substituents to the CTTV molecule may well result in a modified conformation and hence a new, large-bowl host molecule.

Reaction of excess $[\{Ru(\eta^6\text{-}4\text{-}MeC_6H_4CHMe_2)Cl(\mu\text{-}Cl)\}_2]$/$Ag[BF_4]$ with CTTV resulted in the clean formation of a single isomer of the dimetallic species $[\{Ru(\eta^6\text{-}p\text{-cymene})\}_2(\eta^6\text{:}\eta^6\text{-CTTV})][BF_4]_4$ (**11**). Unlike the related complexes of CTV the ^{1}H NMR spectrum of **11** more closely resembles that of a conventional metal−cyclophane species[23] with a singlet resonance for the coordinated ring occurring at a markedly more upfield chemical shift than those for the uncoordinated rings (δ 5.98 and 7.34 ppm, respectively). This trend is also noted for calixarene-based complexes such as $[\{Ru(\eta^6\text{-arene})\}_4(\text{calix[4]arene-2H})]^{6+}$.[9a,b] Also in contrast to the CTV complexes, the protons of the methylenic bridges occur as a poorly resolved multiplet covering a narrow chemical shift range in comparison to the well separated AB resonances for complexes **1**−**10**. These results lead us to suggest that the chair conformation is retained (a bowl conformation should result in a much greater splitting of the signals for the methylenic protons) and indeed, since the ^{1}H NMR spectrum of **11** is sharp at room temperature, exchange between bowl and chair conformations is no longer observed, presumably as a consequence of the large steric bulk of the "$Ru(MeC_6H_4CHMe_2)^{2+}$" substituents. Crystallization of **11** from NO_2Me/Et_2O resulted in yellow needles which rapidly desolvated upon exposure to atmosphere and consequently we were unable to structurally characterize this material.

Twin-Bowl Host. It has been demonstrated that transition metal centers may readily be appended to the outer surface of the CTV molecule. The fact that there are no products with the metal center on the inside of the CTV bowl may readily be attributed to the steric bulk of the arene and Cp* ligands occupying three of the metal coordination sites. In an attempt to generate sandwich-type complexes with the metal center *within* the CTV cavity we have synthesized $[\{Ru(\eta^6\text{-CTV})Cl(\mu\text{-}Cl)\}_2]$ (**12**), the CTV analogue of the chloride bridged starting materials. Treatment of **12** with $Ag[BF_4]$ in acetone as per usual followed by reflux in CF_3CO_2H without addition of any other ligand gave solely a low yield of the *bis*(CTV) species $[Ru(\eta^6\text{-CTV})_2][BF_4]_2$ (**13**), apparently from dimerization of $[Ru(CTV)(acetone)_3]^{2+}$ moieties, followed by elimination of a solvated Ru^{2+} ion. The ^{1}H NMR spectrum of **13** was similar to those observed for other monometallic complexes. Complex **13** was synthesized in much better yield (50%) by reaction of **12**/$Ag[BF_4]$ with additional CTV. The structure of **13**·$6NO_2$-Me is an interesting one from the viewpoint of its inclusion chemistry, since it incorporates both intra-bowl and channel solvent molecules. Four of the six nitromethane molecules adopt the classic channel packing mode,[10] filling the voids between the CTV molecules in the solid state. However, the presence of the bridging transition metal ion precludes the columnar stacking seen in nonmetalated CTV inclusion species and so, as for **1a**, a solvent molecule occupies each CTV cavity with closest guest−host contacts in the region of 3.2 Å. The tetrafluoroborate anions pack outside the CTV cavity on either side of the metal center.

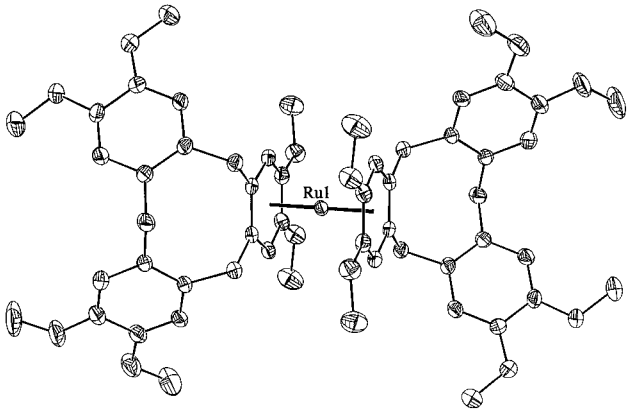

Figure 9. ORTEP plot of the molecular structure of the *bis*(CTV) complex **13**. The included molecule of nitromethane has been omitted for clarity.

Conclusion

It has been demonstrated that by application of simple, well established methodology one, two, or three metal centers may readily be introduced to the outer surface of CTV. The resulting organometallic host molecules display a broad range of solid state inclusion chemistry including (a) channel inclusion of solvent molecules *outside* the CTV cavity as commonly observed for nonmetalated CTV inclusion species, (b) inclusion of neutral guest molecules *within* the CTV bowl as commonly found for other organic hosts such as the calixarenes but not for nonmetalated CTV, and most importantly, (c) inclusion of novel anionic species such as BF_4^-, $CF_3SO_3^-$, $CF_3CO_2^-$, and ReO_4^- within the host cavity, generally in complexes containing at least two transition metal centers. With the exception of our complementary reports of anion inclusion by organometallic calixarene species,[9] this type of anion inclusion within a molecular cavity formed by aromatic rings is without precedent and arises as a direct consequence of the withdrawal of π-electron density by the transition metal centers.

The dimetallic host **4** displays a remarkable ability to complex the large tetrahedral $^{99}TcO_4^-$ and ReO_4^- anions in organic solution. Its selectivity for these anions over chloride, nitrate, sulfate, triflate, and even perchlorate has been demonstrated. Work is in progress on the design of second-generation anion hosts incorporating an even greater degree of anion selectivity based upon cavity size, shape, and functionality considerations.

(19) (a) White, J. D.; Gesner, B. D. *Tetrahedron Lett.* **1968**, 1591. (b) White, J. D.; Gesner, B. D. *Tetrahedron* **1974**, *30*, 2273.

(20) Burlinson, N. E.; Ripmeester, J. A. *J. Inclusion Phenom.* **1985**, *3*, 95.

(21) Zhang, H.; Steed, J. W.; Atwood, J. L. *Supramol. Chem.* **1995**, *4*, 185.

(22) Barbour, L. J.; Steed, J. W.; Atwood, J. L. *J. Chem. Soc., Perkin Trans. 2* **1995**, 857.

(23) (a) Elsegood, M. R. J.; Steed, J. W.; Tocher, D. A. *J. Chem. Soc., Dalton Trans.* **1992**, 1797. (b) Steed, J. W.; Tocher, D. A. *J. Chem. Soc., Dalton Trans.* **1993**, 3187. (c) Swann, R. T.; Hanson, A. W.; Boekelheide, V. *J. Am. Chem. Soc.* **1986**, *108*, 3324.

Experimental Section

Instrumental. NMR spectra were recorded either on a Bruker ARX-250 spectrometer operating at 250.1 (^{1}H) and 62.9 MHz (^{13}C), a Bruker DRX-500 operating at 500.1 (^{1}H) and 125.8 MHz (^{13}C), or a Nicolet NT-200 instrument (200 MHz, ^{1}H). Infrared spectra were recorded as Nujol mulls on NaCl plates using a PE710B spectrophotometer while mass spectra were run in fast atom bombardment mode in *m*-nitrobenzyl alcohol matrix at the University of Alabama. Microanalyses for representative compounds were performed by Atlantic Microlabs, Norcross, GA. In many cases attempts to obtain meaningful analytical data were unsuccessful as a result of the varying amounts of solvent molecules loosely retained by these compounds and characterization rests upon ^{1}H NMR, mass spectral, and selected X-ray crystallographic evidence alone. All manipulations except for those explicitly specified could be carried out in air and the products showed no oxygen sensitivity or chemical instability toward moisture, although many new complexes proved to be hygroscopic and tended to lose enclathrated solvent molecules when exposed to the atmosphere.

Radiochemical studies were carried out using a NaI(Tl) solid scintillator well detector with Ortec electronics and windows for counting were set for the isotope of interest. Experiments monitoring more than one γ-emitting isotope were conducted using a GeLi semiconductor detector with Canberra electronics. γ spectra from the GeLi were analyzed using Maestro software from EG&G Ortec, Inc. Energy and efficiency calibrations were based on a Eu-152 standard.

Materials. The chloro complexes [{Ru(η^6-arene)Cl(μ-Cl)}$_2$] (arene = *p*-MeC$_6$H$_4$CHMe$_2$, C$_6$H$_6$ or C$_6$Me$_6$)[13b] and [{Ir(Cp*)Cl(μ-Cl)}$_2$][13c] and cyclotri- and cyclotetraveratrylene were prepared according to published literature procedures.[10b,19] Ruthenium and iridium trichloride hydrates were purchased from Alfa products and RuCl$_3$·*x*H$_2$O (*x* = *ca.* 2) was purified before use by repeated dissolution in water and evaporating to dryness. All other reagents and materials were obtained from the usual commercial sources.

Caution! ^{99}Tc emits a low energy (0.292 MeV) β^- particle with a half-life of 2.12×10^5 years. Although common laboratory glassware provides adequate shielding, normal radiation safety procedures must be used at all times. ^{99m}Tc emits a 140 keV γ-ray with a half-life of 6 h. and ^{188}Re emits a 155-keV γ-ray and a 2.1 MeV β^- with a half-life of 17 h. These should be handled only in a controlled environment by qualified personnel trained in radiation precautions.

The ^{99}Tc was procured from Oak Ridge National Laboratory as ammonium pertechnetate. ^{99m}Tc was eluted from a Mallinckrodt ^{99}Mo/^{99m}Tc generator as sodium pertechnetate. ^{188}Re was eluted as sodium perrhenate from a ^{188}W/^{188}Re generator obtained from the Missouri University Research Reactor (MURR).

Preparations. All preparations of new cationic sandwich complexes, unless otherwise noted, were performed according to the following procedure for **1a** with the appropriate amounts of starting materials specified:

[Ru(η^6-4-MeC$_6$H$_4$CHMe$_2$)(η^6-C$_{27}$H$_{30}$O$_6$)][BF$_4$]$_2$ (1a). The compound [{Ru(η^6-4-MeC$_6$H$_4$CHMe$_2$)Cl(μ-Cl)}$_2$] (0.21 g, 0.34 mmol) was treated with Ag[BF$_4$] (0.28 g, 1.44 mmol) in acetone (15 mL) and the mixture stirred for *ca.* 20 min. The precipitated AgCl was removed by filtration through Celite and the filtrate evaporated to an orange oil. To this oil was added CTV (0.29 g, 0.64 mmol) and the mixture was refluxed in CF$_3$CO$_2$H (*ca.* 15−20 mL) for 1 h. to give a cloudy yellow solution. When cool the mixture was filtered and evaporated to an orange oil. Recrystallization by diffusion of diethyl ether vapour into an acetone solution of this oil resulted in the isolation of the product as yellow needles containing enclathrated water and diethyl ether. Yield 0.53 g, 0.56 mmol, 88%. Anal. Calcd for C$_{37}$H$_{44}$O$_6$B$_2$F$_8$Ru·2H$_2$O: C, 49.63; H, 5.37. Found: C, 49.1; H, 5.1.

[Ru(η^6-4-MeC$_6$H$_4$CHMe$_2$)(η^6-C$_{27}$H$_{30}$O$_6$)][H(CF$_3$CO$_2$)$_2$]$_2$ (1b). [Ru(η^6-4-MeC$_6$H$_4$CHMe$_2$)Cl(μ-Cl)}$_2$] (0.18 g, 0.29 mmol) was refluxed in CF$_3$CO$_2$H (15 mL) for 12 h with CTV (0.086 g, 0.19 mmol) to give a dark orange solution. When cool the mixture was filtered and evaporated to an orange oil. The product was obtained by diffusion of diethyl ether into a 4:1 nitromethane:CF$_3$CO$_2$H solution of the oil. Yield 0.10 g, 0.088 mmol, 46%. Anal. Calcd for C$_{45}$H$_{46}$O$_{14}$F$_{12}$Ru·2H$_2$O: C, 45.96; H, 4.29. Found: C, 45.6; H, 4.4.

[Ru(η^6-4-MeC$_6$H$_4$CHMe$_2$)(η^6-C$_{27}$H$_{30}$O$_6$)][PF$_6$]$_2$ (1c). As for **1a**: [{Ru(η^6-4-MeC$_6$H$_4$CHMe$_2$)Cl(μ-Cl)}$_2$] (0.14 g, 0.23 mmol); Ag[PF$_6$] (0.25 g, 0.99 mmol); CTV (0.10 g, 0.22 mmol). Slow addition of diethyl ether to the reaction mixture resulted in the precipitaion of crude **1c**. The solid was filtered and washed with *ca.* 10 mL of a 9:1 solution of diethyl ether/acteone to yield 0.083 g (0.086 mmol, 22%) of yellow-brown **1c**.

[Ru(η^6-C$_6$H$_6$)(η^6-C$_{27}$H$_{30}$O$_6$)][BF$_4$]$_2$ (2a). As for **1a**: [{Ru(η^6-C$_6$H$_6$)-Cl(μ-Cl)}$_2$] (0.24 g, 0.48 mmol); Ag[BF$_4$] (0.40 g, 2.05 mmol); CTV (0.40 g, 0.89 mmol). After cooling and filtration, addition of diethyl ether to the reaction mixture (50 mL) gave the product as a white solid which was filtered and washed repeatedly with diethyl ether. Yield 0.70 g, 87 mmol, 98%. Anal. Calcd for C$_{42}$H$_{36}$O$_6$B$_2$F$_8$Ru·6H$_2$O C: 49.49; H, 4.75. Found: C, 49.4; H, 4.6.

[Ru(η^6-C$_6$H$_6$)(η^6-C$_{27}$H$_{30}$O$_6$)][H(CF$_3$CO$_2$)$_2$]$_2$ (2b). As for **1a**: [{Ru-(η^6-C$_6$H$_6$)Cl(μ-Cl)}$_2$] (0.15 g, 0.30 mmol); Ag[H$_2$PO$_4$] (0.19 g, 0.93 mmol) in 1:1 acetone/trifluoroacteic acid; CTV (0.08 g, 0.18 mmol). When cool the mixture was filtered and evaporated to a brown oil, which was dissolved in acetone (1 mL). Slow addition of diethyl ether (10 mL) gave the product as a pale yellow, hygroscopic solid. Yield 0.18 g, 0.22 mmol, 61%.

[Ru(η^6-C$_6$Me$_6$)(η^6-C$_{27}$H$_{30}$O$_6$)][BF$_4$]$_2$ (3a). As for **1a**: [{Ru(η^6-C$_6$-Me$_6$)Cl(μ-Cl)}$_2$] (0.40 g, 0.60 mmol); Ag[BF$_4$] (0.47 g, 2.41 mmol); CTV (0.53 g, 1.18 mmol). After cooling and filtration, removal of the solvent and addition of ethanol (5 mL) and diethyl ether (50 mL) gave the product as a white solid. Yield 0.94 g, 1.06 mmol, 90%. Anal. Calcd for C$_{39}$H$_{48}$O$_6$B$_2$F$_8$Ru·H$_2$O: C, 51.73; H, 5.56. Found: C, 51.6; H, 5.3.

[Ru(η^6-C$_6$Me$_6$)(η^6-C$_{27}$H$_{30}$O$_6$)][CF$_3$CO$_2$]$_2$ (3b). As for **1a**: [{Ru(η^6-C$_6$Me$_6$)Cl(μ-Cl)}$_2$] (0.10 g, 0.15 mmol); Ag[H$_2$PO$_4$] (0.13 g, 0.62 mmol) in 1:1 acetone/trifluoroacteic acid; CTV (0.07 g, 0.16 mmol). When cool the mixture was filtered and evaporated to a brown oil, which was dissolved in acetone (1 mL). Slow addition of diethyl ether (10 mL) gave the product as a pale yellow, hygroscopic solid. Yield 0.13 g, 0.14 mmol, 88%.

[Ru(η^6-C$_6$Me$_6$)(η^6-C$_{27}$H$_{30}$O$_6$)][CF$_3$SO$_3$]$_2$ (3c). As for **1a**: [{Ru(η^6-C$_6$Me$_6$)Cl(μ-Cl)}$_2$] (**3c**, 0.28 g, 0.42 mmol) was treated with Ag[CF$_3$-SO$_3$] (0.45 g, 1.75 mmol) in acetone (10 mL) as for **5a**. After filtration through Celite the acetone solution was refluxed in the presence of CF$_3$CO$_2$H (1 mL) with CTV (0.11 g, 0.24 mmol) for 48 h. After cooling and filtration, the mixture was evaporated to an oil and diethyl ether (20 mL) added to give the product as a white solid. Yield 0.15 g, 0.15 mmol, 62%.

[{Ru(η^6-4-MeC$_6$H$_4$CHMe$_2$)}$_2$(η^6:η^6-C$_{27}$H$_{30}$O$_6$)][BF$_4$]$_4$ (4a). As for **1a**: [{Ru(η^6-4-MeC$_6$H$_4$CHMe$_2$)Cl(μ-Cl)}$_2$] (0.15 g, 0.24 mmol); Ag-[BF$_4$] (0.19 g, 0.98 mmol); CTV (0.11 g, 0.24 mmol). Yield 0.21 g, 0.17 mmol, 71%. Anal. Calcd for C$_{47}$H$_{58}$O$_6$B$_4$F$_{16}$Ru$_2$·H$_2$O: C, 43.89; H, 4.70. Found: C, 43.38; H, 4.60.

[{Ru(η^6-4-MeC$_6$H$_4$CHMe$_2$)}$_2$(η^6:η^6-C$_{27}$H$_{30}$O$_6$)][CF$_3$SO$_3$]$_4$ (4b). As for **1a**: [{Ru(η^6-4-MeC$_6$H$_4$CHMe$_2$)Cl(μ-Cl)}$_2$] (0.25 g, 0.41 mmol); Ag[CF$_3$SO$_3$] (0.43 g, 1.7 mmol); CTV (0.18 g, 0.40 mmol). Diffusion of diethyl ether into a nitromethane solution of the oil residue resulted in the isolation of the product as bright yellow needles. Yield 0.51g, 0.34 mmol, 82%.

[{Ru(η^6-4-MeC$_6$H$_4$CHMe$_2$)}$_2$(η^6:η^6-C$_{27}$H$_{30}$O$_6$)][ReO$_4$]$_3$[CF$_3$SO$_3$]·NO$_2$Me (4c). Treatment of [{Ru(η^6-4-MeC$_6$H$_4$CHMe$_2$)}$_2$(η^6:η^6-C$_{27}$H$_{30}$O$_6$)][CF$_3$SO$_3$]$_4$ (**4b**, 0.06 g, 0.04 mmol) with a 2-fold excess of [NBu$^n_4$][ReO$_4$] (0.16 g, 0.32 mmol) in nitromethane (3 mL) followed by slow diffusion of diethyl ether vapor resulted in the isolation of crystals of the product as pale yellow plates which were characterized by X-ray crystallography, IR, and ^{1}H NMR spectroscopy.

[{Ru(η^6-4-MeC$_6$H$_4$CHMe$_2$)}$_3$(η^6:η^6:η^6-C$_{27}$H$_{30}$O$_6$)][BF$_4$]$_6$ (5a). As for **1a**: [{Ru(η^6-4-MeC$_6$H$_4$CHMe$_2$)Cl(μ-Cl)}$_2$] (0.31 g, 0.51 mmol); Ag-[BF$_4$] (0.41 g, 2.11 mmol); CTV (0.10 g, 0.22 mmol). Yield 0.35 g, 0.20 mmol, 91%. Anal. Calcd for C$_{57}$H$_{72}$O$_6$B$_6$F$_{24}$Ru$_3$·5H$_2$O: C, 38.73; H, 4.64. Found: C, 38.9; H, 4.2.

[{Ru(η^6-4-MeC$_6$H$_4$CHMe$_2$)}$_3$(η^6:η^6:η^6-C$_{27}$H$_{30}$O$_6$)][CF$_3$SO$_3$]$_6$ (5b). As for **1a**: [{Ru(η^6-4-MeC$_6$H$_4$CHMe$_2$)Cl(μ-Cl)}$_2$] (0.40 g, 0.65 mmol); Ag[CF$_3$SO$_3$] (0.68 g, 2.65 mmol); CTV (0.05 g, 0.11 mmol). After recrystallization as per **4b** product composition was measured by ^{1}H NMR spectroscopy to contain *ca.* 35% **5b**. Removal of the **4b** contaminant by fractional crystallization yielded 0.094 g (0.045 mmol, 23%) of crystalline, pale yellow **5b**.

[{Ru(η^6-C$_6$H$_6$)}$_3$(η^6:η^6:η^6-C$_{27}$H$_{30}$O$_6$)][BF$_4$]$_6$ (6). As for **1a**: [{Ru-(η^6-C$_6$H$_6$)Cl(μ-Cl)}$_2$] (0.45 g, 0.90 mmol); Ag[BF$_4$] (0.71 g, 3.65 mmol); CTV (0.20 g, 0.44 mmol). After cooling and filtration, the volume of

the filtrate was reduced *in vacuo* to *ca.* 3 cm^3. Addition of diethyl ether (30 mL) gave the product as a pale yellow solid. Yield 0.65 g, 0.43 mmol, 98%. Anal. Calcd for $C_{45}H_{48}O_6B_6F_{24}Ru_3$: C, 35.78; H, 3.18. Found: C, 35.6; H, 3.1.

[Ir(η^5-C_5Me_5)(η^6-$C_{27}H_{30}O_6$)][BF_4]$_2$ (7). As for **1a**: [{Ir(η^5-Cp*)Cl(μ-Cl)}$_2$] (0.12 g, 0.15 mmol); Ag[BF_4] (0.12 g, 0.62 mmol); CTV (0.13 g, 0.29 mmol). The resulting pale yellow solution was filtered and evaporated to *ca.* 2 mL. Slow addition of diethyl ether (30 mL) gave the product as a gray solid. Yield 0.24 g, 0.25 mmol, 86%. Anal. Calcd for $C_{37}H_{45}O_6B_2F_8Ir$: C, 46.70; H, 4.77. Found: C, 46.5; H, 4.9.

[{Ir(η^5-C_5Me_5)}$_2$(η^6:η^6-$C_{27}H_{30}O_6$)][BF_4]$_4$ (8). As for **1a**: [{Ir(η^5-Cp*)Cl(μ-Cl)}$_2$] (0.15 g, 0.19 mmol); Ag[BF_4] (0.15 g, 0.77 mmol); CTV (0.08 g, 0.19 mmol). Dissolution of the resulting oil into NO_2-Me followed by slow addition of diethyl ether yielded the product as a gray powder. Yield 0.12 g, 0.08 mmol, 73%. Recrystallization by diffusion of diethyl ether vapor into a nitromethane solution of the compound gave the product as large, colorless prisms containing *ca.* 1−1.5 molecules of enclathrated diethyl ether. Anal. Calcd for $C_{47}H_{60}O_6B_4F_{16}Ir_2\cdot Et_2O$: C, 40.12, H, 4.62. Found: C, 40.25, H, 4.30.

[{Ir(η^5-C_5Me_5)}$_3$(η^6:η^6:η^6-$C_{27}H_{30}O_6$)][BF_4]$_6$ (9a). As for **1a**: [{Ir(η^5-Cp*)Cl(μ-Cl)}$_2$] (0.20 g, 0.25 mmol); Ag[BF_4] (0.19 g, 1.0 mmol); CTV (0.07 g, 0.16 mmol). After evaporation the resulting oil was recrystallized from NO_2Me/diethyl ether vapor to yield the product as colorless crystals. Yield 0.26 g, 0.13 mmol, 84%. Anal. Calcd for $C_{57}H_{75}O_6B_6F_{24}Ir_3\cdot H_2O$: C, 34.72, H, 3.94. Found: C, 34.09, H, 3.83.

[{Ir(η^5-C_5Me_5)}$_3$(η^6:η^6:η^6-$C_{27}H_{30}O_6$)][CF_3SO_3]$_6$ (9b). As for **1a**: [{Ir(η^5-Cp*)Cl(μ-Cl)}$_2$] (0.12 g, 0.15 mmol); Ag[CF_3SO_3] (0.16 g, 0.62 mmol); CTV (0.04 g, 0.09 mmol). The resulting pale yellow solution was filtered and evaporated to *ca.* 2 mL. Slow diffusion of diethyl ether vapor into the resulting oil resulted in a 3:7 mixture of **9b** and the analogous dimetallic species which was not isolated. Recrystallization by diffusion of diethyl ether vapor into a nitromethane solution of the compound gave pure **9b** as small colorless prisms. Yield 0.03 g, 0.01 mmol, 11%.

[Ru(η^6-4-$MeC_6H_4CHMe_2$){Ir(η^5-C_5Me_5)}$_2$(η^6:η^6:η^6-$C_{27}H_{30}O_6$)]-[BF_4]$_6$ (10). As for **1a**: [{Ir(η^5-Cp*)Cl(μ-Cl)}$_2$] (0.07 g, 0.09 mmol); Ag[BF_4] (0.10 g, 0.51 mmol); [Ru(η^6-4-$MeC_6H_4CHMe_2$)(η^6-$C_{27}H_{30}O_6$)]-[BF_4]$_2$ (**1a**, 0.07 g, 0.08 mmol). The resulting orange-brown solution was filtered and evaporated to *ca.* 2 mL and the product obtained as a white powder by slow diffusion of diethyl ether vapor into the resulting oil. Yield 0.10 g, 0.05 mmol, 63%. Anal. Calcd for $C_{57}H_{74}O_6B_6F_{24}Ir_2Ru\cdot 4H_2O$: C, 35.4; H, 4.27. Found: C, 35.3; H, 3.9.

[{Ru(η^6-4-$MeC_6H_4CHMe_2$)}$_2$(η^6:η^6-$C_{36}H_{40}O_8$)][BF_4]$_4$ (11). As for **1a**: [{Ru(η^6-4-$MeC_6H_4CHMe_2$)Cl(μ-Cl)}$_2$] (0.24 g, 0.39 mmol); Ag-[BF_4] (0.32 g, 1.64 mmol); CTTV (0.10 g, 0.17 mmol). Product is a hygroscopic, pale yellow solid which refused to give agreeable analytical data. Yield 0.08 g, 0.06 mmol, 35%.

[{Ru(η^6-$C_{27}H_{30}O_6$)Cl(μ-Cl)}$_2$] (12). The compound [Ru(η^6-C_6H_6)-(η^6-$C_{27}H_{30}O_6$)][BF_4]$_2$ (**2a**, 0.65 g, 0.81 mmol) was suspended in dry, degassed THF (20 mL). The mixture was stirred for 3 h with a solution of Red-Al in toluene (3.4 M, 1 mL, excess). To the resulting red-brown solution was slowly added degassed water (1 mL) and the mixture pumped to dryness. The resulting black residue was extracted into degassed CH_2Cl_2 (2 × 10 mL) to give a deep yellow solution. Addition of concentrated HCl (0.2 mL) in degassed acetone (5 mL) resulted in the formation of a bright red solution over a period of 5 min. Reduction of the volume of the solvent to *ca.* 2 mL resulted in the deposition of the product as a red-brown solid which was isolated by filtration and washed with diethyl ether. Yield 0.26 g, 0.21 mmol, 52%.

[Ru(η^6-$C_{27}H_{30}O_6$)$_2$][BF_4]$_2$ (13). As for **1a**: [{Ru(η^6-$C_{27}H_{30}O_6$)Cl-(μ-Cl)}$_2$] (**12**, 0.09 g, 0.07 mmol); Ag[BF_4] (0.08 g, 0.41 mmol); CTV (0.06 g, 0.13 mmol). Evaporation to *ca.* 1 mL and treatment with diethyl ether (20 mL) gave the crude product as an off white precipitate. Recrystallization by diffusion of diethyl ether vapor into a nitromethane solution of the compound gave the pure yellow crystalline product. Yield 0.11 g, 0.07 mmol, 50%. Anal. Calcd for $C_{54}H_{60}O_{12}B_2F_8Ru$: C, 55.16; H, 5.14. Found: C, 54.3; H, 5.1.

Solution Binding Studies. Five hundred microliters of a nitromethane solution of **4b** with known molarity (typically 3.0 mM) was added to an equivalent volume of spiked ($^{99m}TcO_4^-$ or $^{188}ReO_4^-$), MO_4^- solution of the same concentration in saline and then vortexed and centrifuged for 10 min. MO_4^- solutions were made from stock saline solutions of ammonium perrhenate (0.114 M) or ammonium pertechnetate (0.101 M). Aliquots were taken from the stock, spiked with tracer (ca. 20 μCi of $^{99m}TcO_4^-$ or 100 μCi of $^{188}ReO_4^-$), and diluted with saline to equal the molarity of **4b**. After centrifuging, aliquots were taken from each layer and counted for activity on the NaI well detector. Timed counts were converted into percent activity in the nitromethane layer. Experiments in which both ^{99m}Tc and ^{188}Re activity was to be counted were performed using a GeLi semiconductor detector. Ratios of the two spiked isotopes were determined. Each experiment was carried out in triplicate.

Competition studies used 0.15 M solutions of $NaNO_3$, Na_2SO_4, and $NaClO_4$ to replace the saline (0.15 M NaCl) used for dilution of the stock solution in the experiments. This produced at least a 20-fold excess of the competitor ion relative to MO_4^-. Extractions were performed as above.

Cyclic Voltammetry. Cyclic voltammograms were recorded in acetonitrile solution with 0.1 M [NBu_4][PF_6] as supporting electrolyte. The solvent was dried and deaerated before use, while the experiment was carried out under a blanket of N_2. A fritted Ag wire in saturated aqueous AgCl solution was used as the reference. The working and counter electrodes were Pt wires connected to an EG & G model 273 potentiostat, interfaced with an IBM compatible personal computer. The effects of junction potentials were neglected. Standard 0.005 M solutions of host complex in acetonitrile containing 0.1 M [NBu_4][PF_6] were prepared, aliquots of 0.1 M solutions of the target anions (as tetrabutylammonium salts) in the same medium were added by syringe in anion:host mole ratios of 1:10, 1:5, 1:2, 1:1, and 2:1, and the changes in the CV relative to the control sample (recorded at the beginning of each run) were monitored.

Crystallography. Crystal data and data collection parameters are summarized in Table 1. Crystals were mounted using silicon grease in thin walled glass capillaries containing a drop of mother liquor where necessary. All crystallographic measurements were carried out with an Enraf-Nonius CAD4 four circle diffractometer equipped either with graphite monochromated Mo Kα or Cu Kα radiation using the $\omega-2\theta$ scan mode. Data sets were corrected for Lorentz and polarization effects and for the effects of absorption (ψ-scans) and crystal decay where appropriate. Structures were solved using the direct methods option of SHELXS-86[24] and developed using conventional alternating cycles of least-squares refinement (SHELXL-76[25] for **1a** and **13**, or SHELXL-93[16]) and difference fourier synthesis. In all cases all non-hydrogen atoms were refined anisotropically except disordered atoms in some isopropyl groups and solvent molecules, while hydrogen atoms were fixed in idealized positions and allowed to ride on the atom to which they were attached. For structures refined with SHELXL-76 all hydrogen atoms were assigned a fixed isotropic displacement factor (U_{iso} 0.08 Å^2), whereas hydrogen atom thermal parameters were tied to those of the atom to which they were attached for those refined using SHELXL-93.[16] All calculations were carried out on an IBM-PC compatible personal computer.

Acknowledgment. We thank the U.S. National Science Foundation for support of this work and gratefully acknowledge the help of Dr. C. D. Hall and Miss T Kim Truong (KCL) for use of the cyclic voltammetric apparatus.

Supporting Information Available: Crystallographic summary for **1a**, **1b**, **3b**, **5a**, **8**, **9a**, and **13** including tables of atomic coordinates and equivalent isotropic displacement parameters, bond lengths and angles, anisotropic displacement parameters, hydrogen atom coordinates, and isotropic displacement parameters as well as full NMR spectra details (78 pages). See any current masthead page for ordering and internet access instructions.

JA961655W

(24) Sheldrick, G. M. *Acta Crystallogr., Sect. A* **1990**, *46*, 467.
(25) Sheldrick, G. M. *SHELX-76*, University of Cambridge, 1976.